第 29 卷 第 2 期
2008 年 2 月
焊 接 学 报
TRANSACTIONS OF THE CHINA WELDING INSTITUTION
Vol. 29 No. 2
February 2008

K418 与 42CrMo 异种金属激光焊接接头组织与力学性能

庞 铭, 虞 钢, 王恒海, 郑彩云
(中国科学院 力学研究所, 北京 100080)

摘 要: 试验研究了额定功率为 3 kW 的连续波 Nd:YAG 激光焊接热输入对激光焊接 K418 与 42CrMo 异种金属焊缝形貌的影响。通过光学显微镜、扫描电镜、能谱分析仪、硬度仪、万能试验机及 X 衍射对激光焊接 K418 与 42CrMo 异种金属焊缝接头组织、元素分布、相组成及接头的力学性能进行分析。结果表明,在焊接热输入恒定的条件下,高功率、高焊速的匙孔焊接比低功率、低焊速的热传导焊接更能增加焊缝熔深。通过扫描电镜在焊缝区域观察到了颗粒状物和针状物,能谱分析表明,颗粒状物 Nb, Ti, Mo 元素聚集, Fe, Ni 元素减少;针状物 Ti, Nb 元素聚集。K418 与 42CrMo 异种金属激光焊接工艺参数优化后的焊缝抗拉强度高于 42CrMo 母材。

关键词: 激光焊接; 热影响区; K418; 42CrMo; 组织
中图分类号: TG456.7 **文献标识码**: A **文章编号**: 0253 - 360X(2008)02 - 0085 - 04

庞 铭

0 序 言

涡轮增压器转子是发动机的核心部件,其质量对发动机的寿命有很大的影响。涡轮增压器转子通常是由 K418 涡轮盘和 42CrMo 涡轮轴焊接而成,二者的热物理性能、高温力学性能差异很大,属于典型的异种金属焊接[1]。K418 是 γ′(Ni_3(Al, Ti))沉淀硬化镍基高温合金,合金中 Al, Ti 元素含量高,焊接时在焊缝区易出现结晶裂纹,在热影响区易出现液化裂纹[2];42CrMo 碳当量质量分数为0.834 %,焊接时具有很强的淬硬倾向,焊接性差[3]。因此把这两种难焊金属焊在一起具有很大的挑战性。目前对 K418 与 42CrMo 异种金属焊接有电子束焊接和摩擦焊焊接。电子束焊接需要真空室和产生 X 射线;摩擦焊焊接接头易产生低应力破坏[4]。

激光焊接具有功率密度大,焊缝热影区小及焊接变形小,且不需要真空室和产生 X 射线。文中研究了激光焊接 K418 与 42CrMo 异种金属焊接热输入对焊缝形貌的影响和焊接接头组织演变规律及接头的力学性能,为激光焊接这两种金属提供理论上的指导。

1 试验方法

材料为镍基铸造高温合金 K418 与合金钢 42CrMo,其化学成分见表 1 和表 2。试验设备采用了连续波 Nd:YAG 固体激光器,额定输出功率 3 kW,光束模式多模,聚焦镜镜头焦距200 mm。侧吹保护气体为高纯度的氩气,侧吹保护气角度 35°,侧吹保护气吹气方向和焊接方向相反。K418 与 42CrMo 采用对接,中间不留间隙,连续激光焊接,激光热源对称性加载在接头中心,焊前用丙酮对试样

表 1 K418 的化学成分(质量分数, %)
Table 1 Chemical composition of K418

C	Cr	Mo	Nb	Al	Ti	Zr	B
0.08～0.16	11.5～13.5	3.8～4.8	1.8～2.5	5.5～6.4	0.5～1.0	0.06～0.15	0.008～0.020
Mn	**Si**	**P**	**S**	**Fe**	**Pb**	**Bi**	**Ni**
≤0.50	≤0.50	≤0.015	≤0.010	≤1.0	≤0.001	≤0.0001	余量

收稿日期: 2007 - 04 - 20

表 2 42CrMo 的化学成分(质量分数, %)

Table 2 Chemical composition of 42CrMo

C	Cr	Mo	Mn	Si	P	S	Fe
0.38～0.45	0.90～1.20	0.15～0.25	0.50～0.80	0.20～0.40	≤0.040	≤0.040	余量

清洗。选用厚度为2 mm的 K418 和 42CrMo 异种金属焊接在热输入(P/v)恒定的条件下,研究激光焊接速度 v 和功率 P 的变化对焊缝形貌的影响。对厚度为3.5 mm厚 K418 与 42CrMo 异种金属激光焊接工艺参数优化后[5],通过线切割切取焊缝横截面,使用王水腐蚀焊缝和 K418,使用硝酸酒精腐蚀 42CrMo。通过光学显微镜和扫描电镜观察焊缝组织;使用能谱仪和 X 衍射分析焊缝区域成分;使用硬度仪和万能试验机测量焊缝区域硬度和焊接接头抗拉强度。

2 结果和分析

2.1 焊缝形貌

图 1 中的焊缝形貌左边是 42CrMo,右边是 K418,在图 1b,c 中的粗线表示焊接接头中心。图 1a 是3.5 mm厚 K418 与 42CrMo 异种金属激光焊接参数优化后的焊缝形貌,其优化参数为激光功率 P = 3 kW,速度 v = 35 mm/s,正离焦1 mm,侧吹保护气流量15 L/min;图 1b,c 是2 mm厚 K418 与 42CrMo 异种金属激光焊接在热输入(P/v)恒定的条件下,其参数为:图 1b 激光功率 P = 1 500 W,速度 v = 40 mm/s,正离焦3 mm,侧吹保护气流量5 L/min;图 1c激光功率 P = 750 W,速度 v = 20 mm/s,正离焦 3 mm,侧吹保护气流量5 L/min。从图 1a 可看出,焊缝表面平整光滑,焊缝深宽比大,为典型的匙孔焊缝形貌。从图 1b 可以看出焊缝的下面为锥形,这说明作用在焊缝正面的激光使材料部分汽化,在焊缝中形成了部分匙孔焊接[6];从图 1c 可以看出焊缝的形貌为弧形,为典型的热传导焊缝形貌[7]。对比图 1b,c 可以看出:在激光焊接热输入相同的条件下,高功率、高速度的匙孔焊接比低功率、低速度的热传导焊接更能增加焊缝熔深。

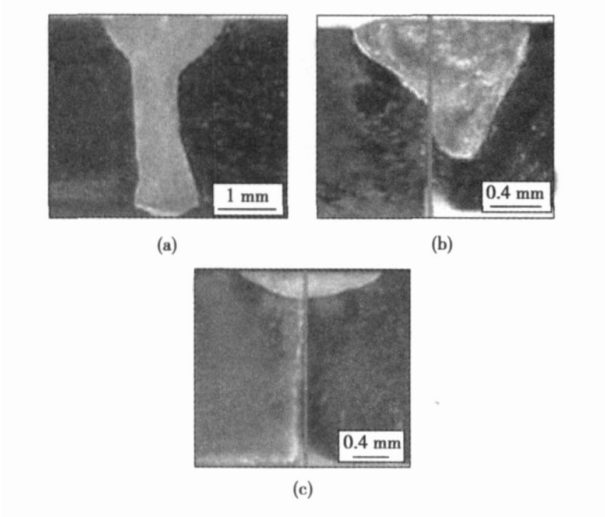

图 1 K418 与 42CrMo 异种金属激光焊接焊缝形貌

Fig. 1 Cross section of K418 and 42CrMo dissimilar metal laser welding

2.2 焊缝组织

图 2 是焊缝区域光学显微镜图。图 2a 是焊缝与 K418 交界;图 2b 是焊缝与 42CrMo 交界。从图 2a,b 可以看出,焊缝与 K418 和 42CrMo 交界的组织为具有一定方向的枝晶组织。

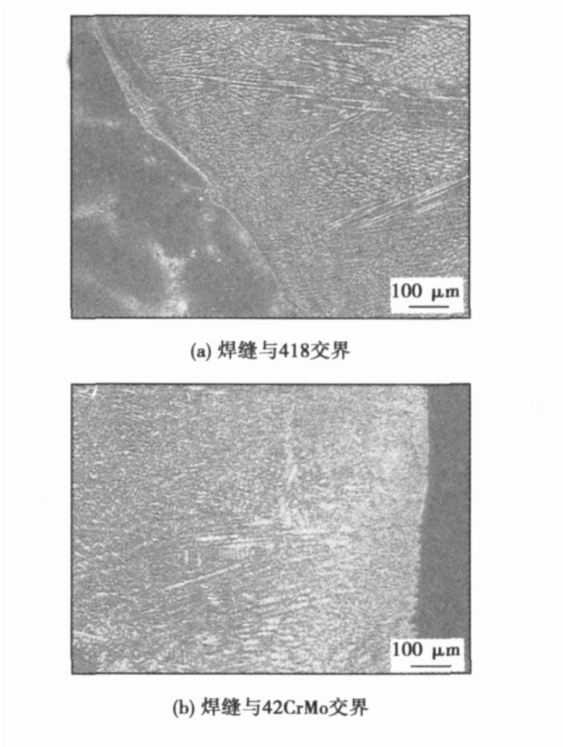

图 2 焊缝组织

Fig. 2 Microstructure of weld

图 3 是焊缝中心扫描电镜图,图 3b 是图 3a 中 A 区的放大图。从图 3a 可以看出:焊缝中心晶粒细小,晶粒细小是由于激光焊接的快速凝固所导致;从图 3b可以看出,在焊缝区弥散分布着颗粒状和针状物。

通过表 3 颗粒状物和针状物与枝晶核的能谱对

比分析表明,颗粒状物 Nb,Ti,Mo 元素聚集,Fe 和 Ni 元素减少;针状物 Nb 和 Ti 元素聚集。

表 3　能谱分析(质量分数,%)

Table 3　EDS analysis results of laser welded seam

	Ni	Fe	Cr	Nb	Ti	Mo	Al
枝晶核	52.450 1	36.499 2	7.146 1	1.569 2	0.203 9	0.705 4	1.426 1
颗粒状	36.850 8	26.108 9	7.911 1	17.394 4	6.129 7	4.279 1	1.325 9
针状	46.354 3	30.215 0	7.138 2	10.023 8	2.802 5	2.015 6	1.450 5

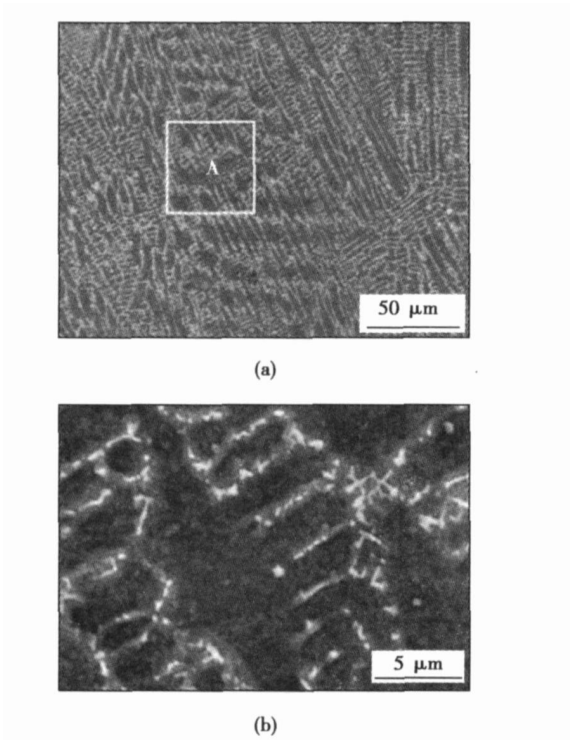

图 3　焊缝扫描电镜图

Fig. 3　SEM photo of weld

图 4 是焊缝区域的 X 衍射。从图 4 可以看出焊缝区的主要相组成是 $FeCr_{0.29}Ni_{0.16}C_{0.06}$,并有微量的 NbC,TiC 和 γ′($Ni_3Al$)。

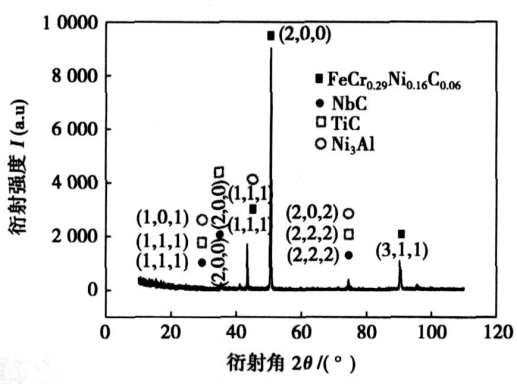

图 4　焊缝区域 X 衍射

Fig. 4　X-ray diffraction result of weld

2.3　接头力学性能

图 5 中 42CrMo 和 K418 侧硬度,是从 42CrMo 和 K418 热影响区一直到母材。从图 5 可以看出,42CrMo 侧热影响区出现了硬化;K418 侧热影响区硬度与母材比波动不大;焊缝区硬度略高于 42CrMo 母材,低于 K418 母材硬度。焊缝区的硬度低于 K418 母材是由于 K418 是镍基铸造高温合金,γ′(Ni_3(Al,Ti))是主要的强化相,激光焊接的快速凝固及熔化的 42CrMo 对 K418 液态金属的稀释的综合作用,使焊缝区域的 γ′分布发生了改变[8]。对优化后的焊缝拉伸试验结果表明,焊接接头强度高于 42CrMo 母材,在拉伸过程中,远离焊缝的基体发生了明显的收缩,如图 6 所示。

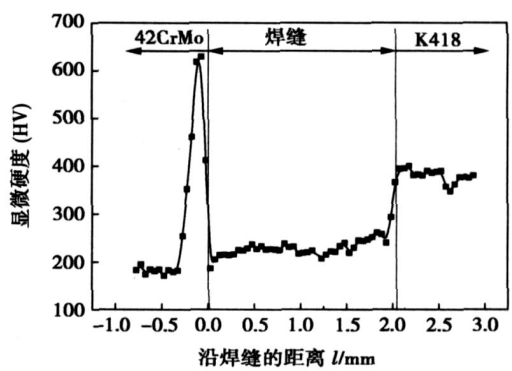

图 5　焊缝区域硬度分布

Fig. 5　Microhadrness distribution along weld

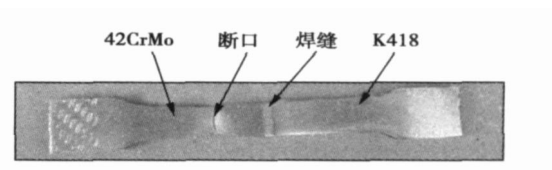

图 6　焊缝拉伸断裂试样

Fig. 6　Fracture weld specimen after tensile testing

3　结　　论

K418 与 42CrMo 异种金属激光焊接由于它们热

物理性质的差异,对称性的热源加载在接头中心产生了非对称性的熔池。在激光焊接热输入恒定的条件下,高功率、高焊速的匙孔焊接比底功率、低焊速的热传导焊接更能增加焊缝熔深。XRD 分析表明,焊缝区的主要物相是 $FeCr_{0.29}Ni_{0.16}C_{0.06}$,并有微量的 NbC,TiC 和 γ′。K418 与 42CrMo 异种金属激光焊接优化工艺参数后的焊缝的抗拉强度高于 42CrMo 母材。

参考文献:

[1] Lee J W. Inertia friction welding of a gas turbine rotor[J]. Welding Review International,1992,11 (4):189 - 192.

[2] Zhong Minlin, Sun Hongqing, Liu Wenjin, *et al*. Boundary liquation and interface cracking characterization in laser deposition of Inconel 738 on directionally solidified Ni-based superalloy[J]. Scripta Materialia,2005,53:159 - 164.

[3] 夏伟白. 42CrMo 中碳调质高强钢的焊接[J]. 电焊机,1989,5:30 - 31.

[4] 杜随更,傅 莉,曹 营,等. K418 涡轮盘和 42CrMo 轴摩擦焊接头的强化[J]. 西北工业大学学报,2004,22(1):112 - 115.

[5] 庞 铭,虞 钢,刘 兆,等. K418 与 42CrMo 异种金属的激光穿透焊接[J]. 中国激光,2006,33(8):1122 - 1126.

[6] Phanikumar G, Dutta P, Chattopadhyay K. Continuous welding of Cu-Ni dissimilar couple using CO_2 laser[J]. Science and Technology of Welding and Joining,2005,10(2):158 - 166.

[7] 虞 钢,虞和济. 集成化激光智能加工工程[M]. 北京:冶金工业出版社,2001.

[8] Sekhar N C, Reed R C. Power beam welding of thick section nickel base superalloys[J]. Science and Technology of Welding and Joining, 2002,7(2):77 - 87.

作者简介:庞 铭,男,1980 年出生,博士研究生。主要从事激光焊接试验与数值模拟研究。发表论文 3 篇。

Email: pangming@imech.ac.cn

[上接第 12 页]

深增加的原因是焊剂对光束吸收率的提高以及焊剂改变了熔池的流动模式。

参考文献:

[1] 单际国. 聚焦光束钎焊及表面改性技术研究[R]. 北京:清华大学,1998.

[2] 张 涛. 低碳钢薄板聚焦光束焊接工艺的研究[D]. 北京:清华大学,2003.

[3] Gurevich S M, Zamkov V N. Increase in melting efficiency of titanium alloy in TIG welding[J]. Avtomaticheskaya Svarka, 1965(9): 1 - 4.

[4] Herple C R, Roper J R. Mechanism for minor element effect on GTA fusion zone geometry[J]. Welding Journal, 1982, 61(4): 97s - 102s.

[5] Heiple C R, Roper J R, Stagner R T, *et al*. Surface active element effects on the shape of GTA, laser and electron beam welds[J]. Welding Research Supplement, 1983, 62 (3): 72 - 77.

[6] 单际国, 张 涛, 任家烈. 氧化物活性焊剂对低碳钢聚焦光束焊接熔深的影响[J]. 焊接, 2006(4): 21 - 24.

[7] 中国科学院数学研究所数理统计组. 正交试验法[M]. 北京: 人民教育出版社, 1975.

[8] 张 迪. 光束堆焊反应合成 NiAl 化合物层的组织特征及其形成机理[D]. 北京: 清华大学, 2005.

[9] Lu Shanping, Fujii Hidetoshi, Sugiyama Hiroyuki, *et al*. Weld penetration and marangoni convection with oxide fluxes in GTA welding[J]. Materials Transactions, 2002, 43(11): 2926 - 2931.

作者简介:单际国,男,1965 年出生,工学博士,教授,博士生导师。主要从事激光焊接、堆焊等方面的工作。发表论文 60 余篇。

Email: shanjg@tsinghua.edu.cn

under low heat input ZHANG Fuju[1] , WANG Yan[2] , ZHANG Guodong[1] , Wang Yutao[3] (1. College of Power & Mechanical Engineering , Wuhan University , Wuhan 430072 , China ; 2. College of Mechanical & Material Engineering , China Three Gorges University , Yichang 443002 , Hubei , China ; 3. Research Institute of Wuhan Iron & Steel Group Corporation , Wuhan 430080 , China) . p77 - 80

Abstract : The formation and mechanical properties of welded joint for 400 MPa ultra-fine grain steel were studied based on surface tension transfer technology , CO_2 arc welding , special narrow groove and different heat input. The results showed that the welded joint with good fusion , one side welding with back formation and narrow HAZ (heat-affected zone) (about 1 mm) was obtained with 3-4 kJ/cm heat input. The hardness and tensile strength of the joint were higher than those of the base metal. The embrittlement and softening of HAZ was not found , and the bending plasticity was qualified. The impact toughness of HAZ was about 60 % higher than that of the base metal , which can be caused by the granular pearlite transition , multi-phase non-equilibrium microstructure and higher yield stress.

Key words : ultra-fine grain steel ; welded joint ; heat input ; CO_2 arc welding

Residual stress and distortion of Al alloy panels welded by FSW LI Hongke , SHI Qingyu , WANG Xin , LI Ting , LIU Yuan (Department of Mechanical Engineering , Key Laboratory for Advanced Materials Processing Technology Ministry of Education , Tsinghua University , Beijing 100084 , China) . p81 - 84

Abstract : FSW 6056-T6 Al alloy panel was welded by FSW and its distortion was measured. Also numerical model was established to simulate the distortion , temperature field and stress fields. The simulated temperature and distortion were compared with those of experiments. The results indicated that the panel bent down along welding direction and maximum distortion reaches 6. 3 mm. Along the transverse direction , the panel bent up relatively to the longitudinal sides and the maximum displacement was 4. 5 mm. There were high accordance trends of simulated distortion to the experiment. The longitudinal residual stress was asymmetric with the weld center line and it is higher on advancing side.

Key words : friction stir welding ; welding distortion ; numerical simulation

Microstructure and mechanical properties of K418 and 42CrMo dissimilar metal laser welding PANG Ming , YU Gang , WANG Henghai , ZHENG Caiyun (Institute of Mechanics , Chinese Academy of Sciences , Beijing 100080 , China) . p85 - 88

Abstract : The influences of welding heat input on weld of laser welding of K418 and 42CrMo dissimilar metal were experimentally investigated using continue wave Nd : YAG laser of output power 3 kW. Microstructure of the welded joint was studyed by optical microscope , scanning electron microscope , X-ray diffraction , and energy dispersive spectrometer. Mechanical properties of the weld were evaluated by hardness and tensile strength test. Results show that weld penetration of keyhole welding mode is larger than of heat conduction welding mode with constant linear heat input. Particle of rich Nb , Ti and Mo and deleted Fe and Ni and needle of rich Nb and Ti are observed in the fusion zone. The tensile strength of weld is higher than that of base metal of 42CrMo by optimizing laser welding parameters.

Key words : laser welding ; heat-affected zone ; K418 nickel alloy ; 42CrMo steel ; microstructure

Weld defect classification in ultrasonic testing basing on time-frequency discriminant features DU Xiuli[1,2] , SHEN Yi[2] , WANG Yan[2] (1. School of Information Engineering , Dalian University , Dalian , 116622 , China ; 2. School of Astronautics , Harbin Institute of Technology , Harbin 150001 , China) . p89 - 92

Abstract : According to transient property of ultrasonic signal , the discriminant pursuit method was proposed to extract local time-frequency features of defect signal and the features were fed to a probabilistic neural networks to classify the defects. During extracting features , the correlation between the incoming atom and the atoms selected before was considered to reduce the redundance among the selected atoms so that the extracted features discriminated different class of signals effectively. Finally , the defects of an electronic welded joint were classified by proposed approach , and the experimental results show that time-frequency discriminant features are appropriate for defects classification in ultrasonic testing , and can suppress the effect of grain noise. In addition , the higher accuracy can be reached if considering the correlation of the selected atoms.

Key words : ultrasonic test ; discriminant pursuit ; time-frequency discriminant feature ; probabilistic neural networks

Prediction of area of gray-spots flaw in alternate rail flash butt welded joint based on RBF neural network LÜ Qibing , TAN Keli , LUO Deyang , TAN Hongtao (Institute of Welding , Southwest Jiaotong University , Sichuan Chengdu 610031 , China) . p93 - 96

Abstract : On the basis of imported AMS60 alternate rail flash butt welding machine , the welding current , the welding voltage and the displacement of welding procedure experiment of U71Mn rail were acquired with high frequency. Eight weld quality characteristic values such as the percentage of the flashing time of the accelerated flashing stage , the percentage of the flashing time of low voltage Ⅱ and stable flash stage , the power input of weld , the flashed length of rail , the welding time , the short and broken circuit factor of low voltage Ⅱ and stable flash stage and the short and broken circuit factor of the accelerated flashing stage and upsed length , which had influence on the grey-spot flaw area in the alternate rail flash butt welded joint , were used as input data of radial basic function neural network the rail weld grey-spot flaw. The prediction model whose spread rate was 1. 5 was built , and according to the TB/ T1632 -